Origin of functional diversity among tetrameric voltage-gated channels

ARTICLE *in* PROTEINS STRUCTURE FUNCTION AND BIOINFORMATICS · OCTOBER 2006

Impact Factor: 2.63 · DOI: 10.1002/prot.21187 · Source: PubMed

3 AUTHORS:

Claudio Anselmi
National Heart, Lung, and Blood Institute
46 PUBLICATIONS **863** CITATIONS
SEE PROFILE

Paolo Carloni
Forschungszentrum Jülich
276 PUBLICATIONS **5,974** CITATIONS
SEE PROFILE

Vincent Torre
Scuola Internazionale Superiore di Studi Ava…
231 PUBLICATIONS **8,135** CITATIONS
SEE PROFILE

PROTEINS: Structure, Function, and Bioinformatics 66:136–146 (2007)

Origin of Functional Diversity Among Tetrameric Voltage-Gated Channels

Claudio Anselmi, Paolo Carloni, and Vincent Torre*
Istituto Nazionale per la Fisica della Materia (INFM-DEMOCRITOS Modelling Center for Research in Atomistic Simulation) and International School for Advanced Studies (SISSA), Trieste I-34014, Italy

ABSTRACT **The aim of the present work is to relate functional differences of voltage-gated K^+ (K_v), hyperpolarization-activated cyclic nucleotide-gated (HCN), and cyclic nucleotide gated (CNG) channels to differences in their amino acid sequences. By means of combined bioinformatic sequence analyses and homology modelling, we suggest that: (1) CNG channels are less voltage-dependent than K_v channels since the charge of their voltage sensor, the S4 helix, is lower than that of K_v channels and because of the presence of a conserved proline in the S4–S5 linker, which is quite likely to uncouple S4 from S5 and S6. (2) In HCN channels, S4 features a higher net positive charge with respect to K_v channels and an extensive network of hydrophobic residues, which is quite likely to provide a tight coupling among S4 and the neighboring helices. We suggest insights on the gating of HCN channels and the reasons why they open with membrane hyperpolarization and with a significantly longer time constant with respect to other channels. Proteins 2007;66:136–146.** © 2006 Wiley-Liss, Inc.

Key words: voltage-gated ionic channels; CNG and HCN channels; comparative modeling; channel intracellular gating; structural models; low homology

INTRODUCTION

Na^+, K^+ and, Ca^{2+} ion channels,[1] the most well known members of the superfamily of voltage-gated ion channels,[2] open in less than 1 or 2 ms when the membrane potential is depolarized from its resting level around −50 to about 0 mV.[3] These channels play a crucial role in several major physiological processes, such as the generation of nerve impulses, synaptic release, and muscle contraction.

The transmembrane domains of these channels exhibit different folds. Voltage-gated K^+ channels (K_v channels) are tetramers, each subunit featuring a six-transmembrane-helix (S1–S6) bundle [Fig. 1(A)]. Between the S5 and S6 helices, there is a pore region formed by a short helix referred to as P-helix and the inner pore constituted by a short stretch of amino acids.[4] The S4 domain is characterized by the repeat of the triplet a^+bc, where the amino acid in position a^+ is either a lysine or an arginine, whereas in positions b and c there are hydrophobic amino acids. Therefore, S4 is thought to be acting as the voltage sensor.[5–11] The recent determination of the X-ray structure of $K_v1.2$ from the rat[10,11] has provided the structural determinants of K_v channels in the open conformation. The position of S4 explains a large number of experimental observations,[12–14] which could not be reconciled with an earlier three-dimensional (3-D) structure of a prokaryotic K^+ channel,[9] and supports the notion that during gating the S4 domain has a small vertical motion of just a few angstroms.[12,13]

By contrast, Na^+ and Ca^{2+} channels are monomers containing four internal repeats, evolved from K^+ channels through two gene duplications.

The voltage-gated channel superfamily also includes other subfamilies, whose members share the same transmembrane topology of K_v channels,[15–17] but show a large cytoplasmic cyclic nucleotide binding (CNB) domain, composed of several hundreds of amino acids and connected to the S6 domain [Fig. 1(B)]: cyclic nucleotide gated (CNG) channels and hyperpolarization-activated cyclic nucleotide-gated (HCN) channels. CNG channels from photoreceptors and olfactory sensory neurons are crucial for the conversion of external stimuli into changes of membrane potential.[18–20] They are very poorly voltage dependent and require the presence of micromolar amounts of cyclic nucleotides (such as cyclic adenosine monophosphate (cAMP) or cyclic guanosine monophosphate (cGMP)) in order to open in a time scale of the order of 1 or 2 ms.[21] HCN channels play a role in controlling heartbeat and neuronal rhythmic activity.[22–25] They open within 100 ms or so, when the membrane potential hyperpolarizes below −60 mV and often at lower voltages than −100 mV.[1] HCN channels are also regulated by cAMP, which accelerates the activation kinetics and shifts the channel opening to more positive potentials.[21,26]

Grant sponsors: MIUR COFIN 2004 (Ministero dell'Università e della Ricerca), HFSP (Human Frontier Science Program), GRAND (FVG/CIPE).

*Correspondence to: Vincent Torre, Istituto Nazionale per la Fisica della Materia (INFM-DEMOCRITOS Modelling Center for Research in Atomistic Simulation) and International School for Advanced Studies (SISSA), Via Beirut, 2-4, Trieste I-34014, Italy.
E-mail: torre@sissa.it

Received 3 April 2006; Revised 28 June 2006; Accepted 19 July 2006

Published online 16 October 2006 in Wiley InterScience (www.interscience.wiley.com). DOI: 10.1002/prot.21187

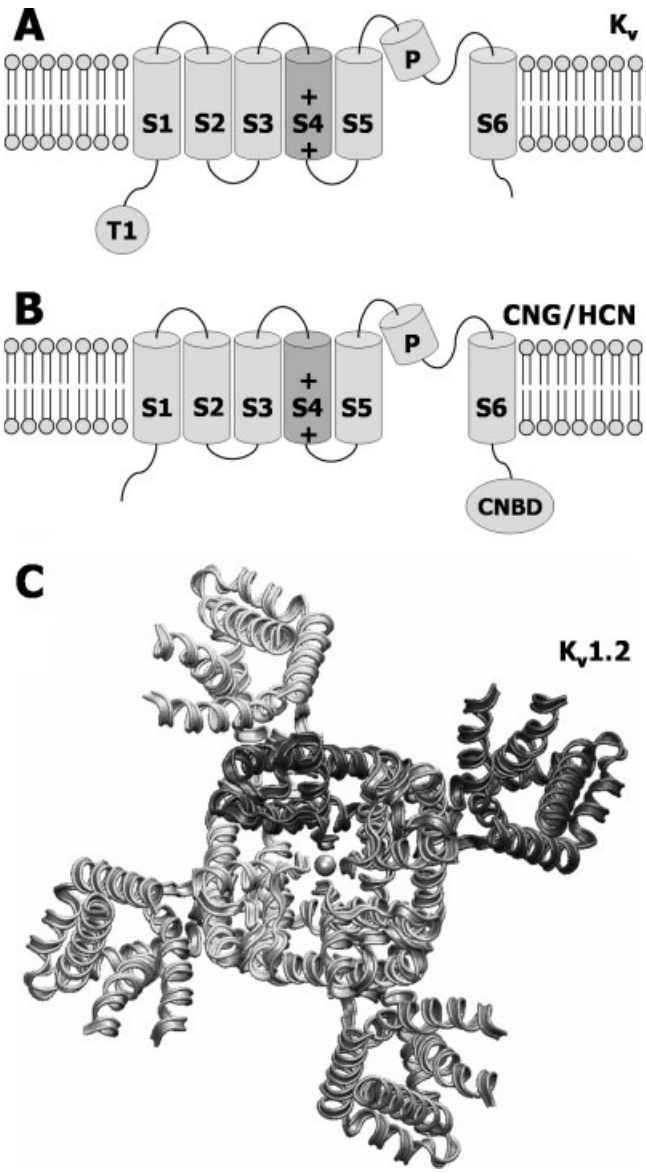

Fig. 1. Comparison between the topology of K_v, CNG, and HCN K^+ channel subunits. The biological molecules of all these channels are constituted by tetramers. (**A**) K_v channels consist of six transmembrane helices, a P loop, and the selectivity filter. Generally, a large T1 domain is bound to the N-terminal part. (**B**) CNG and HCN channels share the same pore topology of K_v channels, but their C-terminal domain is bound to a large cyclic nucleotide binding domain (CNBD), whereas T1 is absent. (**C**) Top view of the crystallographic structure of K_v1.2.[10,11]

K^+, HCN, and CNG channels show different ion selectivity properties in a marked way. K^+ channels are permeable primarily to K^+ and Rb^+ ions and at a lesser extent to Cs^+ and Tl^+ ions. By contrast, HCN channels are permeable also to Na^+ ions but are blocked by Cs^+ ions. CNG channels are permeable to all monovalent alkali cations (Li^+, Na^+, K^+, Rb^+, and Cs^+), to a variety of small organic cations, and to some divalent cations, such as Ca^{2+}, Mg^{2+}, Sr^{2+}, and Mn^{2+}. On the contrary, K^+ and HCN channels are not permeable to any organic compound and are clearly more selective than CNG channels.[1] This functional difference is very likely ascribed to the presence of the GYG motif in the pore of K^+ and HCN channels, which is indeed replaced by a single glycine in CNG channels.[27] Therefore, the pore of K^+ and HCN channels is longer and consequently more selective. The recent structural determination of a Na^+- and K^+-conducting channel could cast more light on the structural differences in the selectivity filter, which result in the loss of ion selectivity in CNG channels.[28] Moreover, the flexibility of the pore region of HCN channels is quite likely to be higher than in K^+ channels, probably playing a role for the lower selectivity of these channels with respect to the others.[29]

To date, it is believed that the open conformation of all these channels is associated to an outward bending of the S6 domain and, possibly, to an anticlockwise rotation in CNG channels.[30] The hinge is identified with the PXP motif in K_v channels[31–35] and with a glycine residue in HCN and CNG channels.[27,29,36–38] In K_v channels, the S4 domain moves up following membrane depolarization allowing S6 bending.[4,11–13,39] The same behavior is also shown by the S4 domain of HCN channels.[8] Therefore, the fact that S4 helix moves up following membrane depolarization ("up" conformation) and down following membrane (hyper)polarization ("down" conformation) seems common among K^+ channels.

Here, we use bioinformatic tools, combined with the analysis of K_v1.2 structure,[10,11] to relate functional diversity of tetrameric voltage-gated channels to differences in their amino acid sequences. Specifically, we provide structural insights on the different gating mechanisms of K_v, HCN and CNG channels.

MATERIALS AND METHODS

The crystal structures of six different potassium channels have been recently solved: KcsA[40] (PDB entry: 1K4D),[41] KirBac1.1 (PDB entry: 1P7B),[42] MthK (PDB entry: 1LNQ),[37,38] NaK (PDB entry: 2AHZ),[28] K_vAP (PDB entry: 1ORQ),[9] and K_v1.2 (PDB entry: 2A79).[10,11] The first four channels have two-transmembrane-helix topology whereas the other channels have six transmembrane helices. The 3-D structure of the inner pore comprising two transmembrane helices and the P-helix of all these channels is remarkably similar, with a RMSD less than 2.0 Å in spite of the low amino acid homology. To use this structural information, we first constructed the structural alignment of the channel inner pore regions with the STAMP program.[43] As the cluster containing all the six initial structures had a low score, the best cluster contained MthK, NaK and the S5–S6 helices and the P helix of K_vAP and K_v1.2, having a root mean square deviation of 1.7 Å. The corresponding structural alignment was then used as starting block for the multiple alignment of all considered HCN and CNG channels (the related notations are reported in the legend of Fig. 2). Alignments were performed by means of the MULTI-

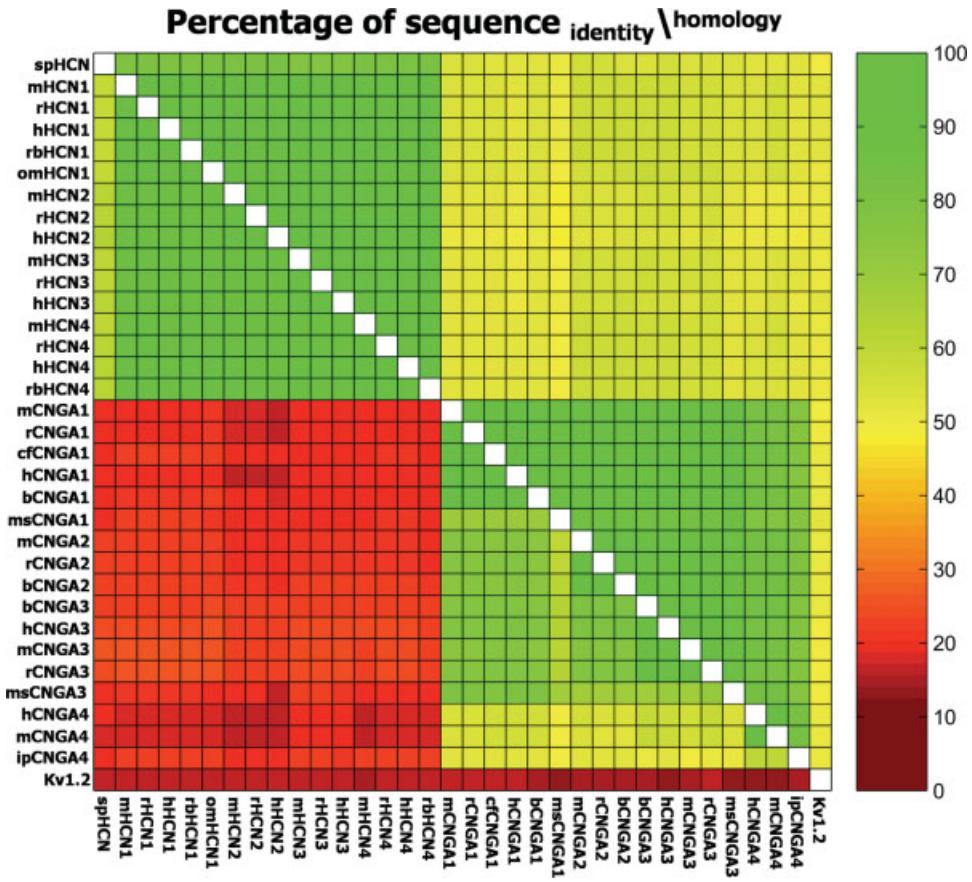

Fig. 2. Percent sequence identity and sequence homology among different ion channels in the regions from S3 to S6. As for the channel notation, the first letter(s) of the name represent the organism of origin (sp, *S. purpuratus* (sea urchin); m, *M. musculus* (mouse); r, *R. norvegicus* (rat); h, *H. sapiens* (human); rb, *O. cuniculus* (rabbit); om, *O. mykiss* (rainbow trout); cf, *C. familiaris* (dog); b, *B. taurus* (bovine); ms, *M. saxatilis* (striped bass); ip, *I. punctatus* (channel catfish)). The corresponding database entries are the following (sp: SWISS-PROT; tr: trEMBL): spHCN, trO76977; mHCN1, spO88704; rHCN1, spQ9JKB0; hHCN1, spO60741; rbHCN1, spQ9MZS1; omHCN1, trQ71N53; mHCN2, spO88703; rHCN2, spQ9JKA9; hHCN2, spQ9UL51; mHCN3, spO88705; rHCN3, spQ9JKA8; hHCN3, spQ9P1Z3; mHCN4, spO70507; rHCN4, spQ9JKA7; hHCN4, spQ9Y3Q4; rbHCN4, spQ9TV66; mCNGA1, spP29974; rCNGA1, spQ62927; cfCNGA1, spQ28279; hCNGA1, spP29973; bCNGA1, spQ00194; msCNGA1, trQ3I0N0; mCNGA2, spQ62398; rCNGA2, spQ00195; bCNGA2, spQ03041; bCNGA3, spQ29441; hCNGA3, spQ16281; mCNGA3, spQ9JJZ8; rCNGA3, trQ9ER33; msCNGA3, trQ3I0N2; hCNGA4, trQ3B859; mCNGA4, trQ3UW12; ipCNGA4, trQ8JFP0; K_v1.2, spP63142. [Color figure can be viewed in the online issue, which is available at www.interscience.wiley.com.]

ALIGN program[44,45] using standard parameters and adopting secondary structure-dependent gap penalty.[46]

Prediction of secondary structure elements was performed using the PSIPRED server.[47] Amino acid solvent accessible surface areas were calculated by means of the NACCESS program[48] starting from the channel 3-D structures. We considered amino acids as buried when less than 30% of their total area was exposed to the solvent.

Partial 3-D structural models were built for spHCN, mHCN2, and bCNGA1 channels, because they are representative of their respective channel subfamilies, given the high internal sequence homology (Fig. 2). With this aim, the MODELLER 6.2 program[49] was used, adopting the crystallographic structure of rat K_v1.2[10,11] as a template.

As for CNG channels, we just considered channel subunits CNGA1–4.[50–54] In fact, CNGA1–3, generally referred to as α subunits, form homotetrameric functional channels,[50] whereas the other known subunits,[55,56] referred to as β subunits, are functionally inactive. The CNGA4 subunit could be considered as a β subunit, because CNGA4 homotetramers are functionally inactive,[53,54] but it is more similar to CNGA1–3 subunits,[57] and the replacement of the first 78 amino acids of the C-linker region with the corresponding residues from an α subunit is sufficient to yield functional chimeric subunits.[58]

To validate the initial alignment, we checked if the related structural models are compatible with the experimental data. Specifically, in the bovine homotetrameric CNG channel (bCNGA1), application of the oxidizing agent copper phenantroline in the open state locks the mutant channel F380C in this state.[27] This effect is abolished in the double mutant F380C&C314S, support-

ing the hypothesis that F380 in S6 is spatially close to native C314 in S5 (at least in the open state). In spHCN, application of Cd^{2+} ions locks the mutant channel H462C&L466C in the open state.[29] This experimental evidence supports the hypothesis that H462 and L466, located in S6, are spatially close in the open state to native C369 and C373, located in S5, to form a binding site for a Cd^{2+} ion.[29] Both restraints are satisfied in the homology models of the corresponding channels.

Unfortunately, the great majority of experimental electrophysiological data are confined between the S5 and the S6 domains. Therefore, the structural models we considered are limited to the S5–S6 tract for HCN channels, whereas in the case of CNG channels, we built models for the S4–S6 tract imposing conformational restraints[49] to the S4–S5 linker region (see the following section).

RESULTS AND DISCUSSION

The recently determined crystal structure of $K_v1.2$[10,11] makes it the most obvious template for building homology models of HCN and CNG channels. Models provide a way for understanding the spatial arrangement of key residues in these channels and for hypothesizing possible molecular interactions between different domains responsible for their gating. Our analysis is restricted to residues located between the S3 and S6 domains, since sequence homology in other regions is very low, and presumably they are also less functionally relevant for gating. As shown in Figure 2, HCN channels have a very high amino acid identity among themselves (between 58 and 100%), but lower with CNGA1–4 and $K_v1.2$ channels (17–24%, and 15–17%, respectively). The amino acid identity among $K_v1.2$ and CNGA1–4 channels is between 13 and 16%. Equivalent conclusions are obtained when sequence homology is considered.

Figure 3 illustrates the sequence alignment of sea urchin HCN, the mouse HCN1–4 channels, the bovine CNGA1–3 channels, human CNGA4, and rat $K_v1.2$ in the S3–S6 region. In fact, given the very high sequence homology among these channels in different organisms (generally higher than 90%), they could be chosen as a representative subset of the ionic channels under investigation. We also reported the secondary structure annotation of $K_v1.2$, derived from the crystallographic structure, and the relative buried amino acids (black arrows). Moreover, the figure contains information, which will be discussed later in the text: the conserved glycines in S5 and S6 domains (red arrows), the conserved F459 (spHCN notation; blue arrow), and P293 (bCNGA1 notation; yellow arrow). In addition, amino acids with high occurrence in α-helical interfaces of membrane proteins are reported in different colors.

A recent analysis[59] has highlighted that soluble and membrane helix bundles show different preferences for amino acids at α-helical interfaces. In soluble α-bundle proteins, the most important residues for tight helix packing are Ala, Leu, Ile, and Val, which have high occurrences at the "*a*" and "*d*" positions of patterns (*abcdefg*), generally called "coiled-coils" motifs.[60,61] In fact, being the α-helix periodicity equal to 3.6 residues per turn, amino acids in positions "*a*" and "*d*" of heptad repeats face toward the same direction, forming an interface for another α-helix. In membrane protein, common interfacial amino acids are Ala, Gly, Leu, Ile, Phe, Ser, Thr, and Val.[59] However, whereas Ala, Gly, and Ser (shown in red in Fig. 3) have a very high propensity for interfaces between α-helices with a short backbone separation (≤6 Å), Leu, Ile, Thr, and Val (shown in purple) tend to be present at interfaces between more distant α-helices. Phe (shown in yellow) is common at the α-helix interfaces, but have a higher propensity for noninterfacial position, pointing toward the membrane.[59]

To verify the significance of Ala, Gly, Leu, Ile, Phe, Ser, Thr, and Val for helical interfaces and further validate the alignment, we checked if conserved positions in the alignment (namely positions in which at least 60% of the residue are putative interfacial amino acids) actually correspond to amino acid at α-helical interfaces. As a representative parameter, we calculated the total of the exposed surface area of every residue in $K_v1.2$ crystal structure. In the tract S5–S6, which is expected to be more structurally similar between channels, 66 buried residues are present (black arrows in Fig. 3), whose 68% corresponds to conserved positions. By contrast, only 12 conserved positions correspond to exposed residues. Therefore, the occurrence of Ala, Gly, Leu, Ile, Phe, Ser, Thr, and Val in conserved positions and the presence of the amino acids at α-helical interfaces are strongly correlated. In the region from S3 to S6, 67% of the buried residues still match conserved positions, but there are 27 conserved positions, which correspond to exposed residues in $K_v1.2$. This further supports the hypothesis that $K_v1.2$, HCN, and CNG channels are more structurally divergent in the S3–S4 tract than in the S5–S6 tract.

Presence of Amino Acids with High Interfacial Propensity

A remarkable difference among the three channel subfamilies is that S4 and the lower part of S5 domains of HCN channels feature the presence of residues with a high α-helix interface propensity, in particular Leu and Ser, at highly conserved locations and forming heptad repeats (Fig. 3). The presence of these residues highly suggests a tight helical coupling between the S4 and S5 domains of HCN channels. As aforementioned, Ser is one of the amino acids with the highest propensity for interfaces between α-helices with a tight packing.[59] Leu is the most abundant residue at α-helix interfaces and it is able to form motifs, called leucine zippers,[62] which stabilize α-helix interactions. The substitution of conserved leucines in heptad repeats of the Shaker channel family resulted in alterations of the voltage-dependence of the channel opening, supporting the hypothesis that gating conformational changes could be mediated by leucine interactions.[63] Finally, leucine role in the gating of HCN channels is also supported by the recent electrophysiological experiments on spHCN.[64] This channel rapidly deactivates following

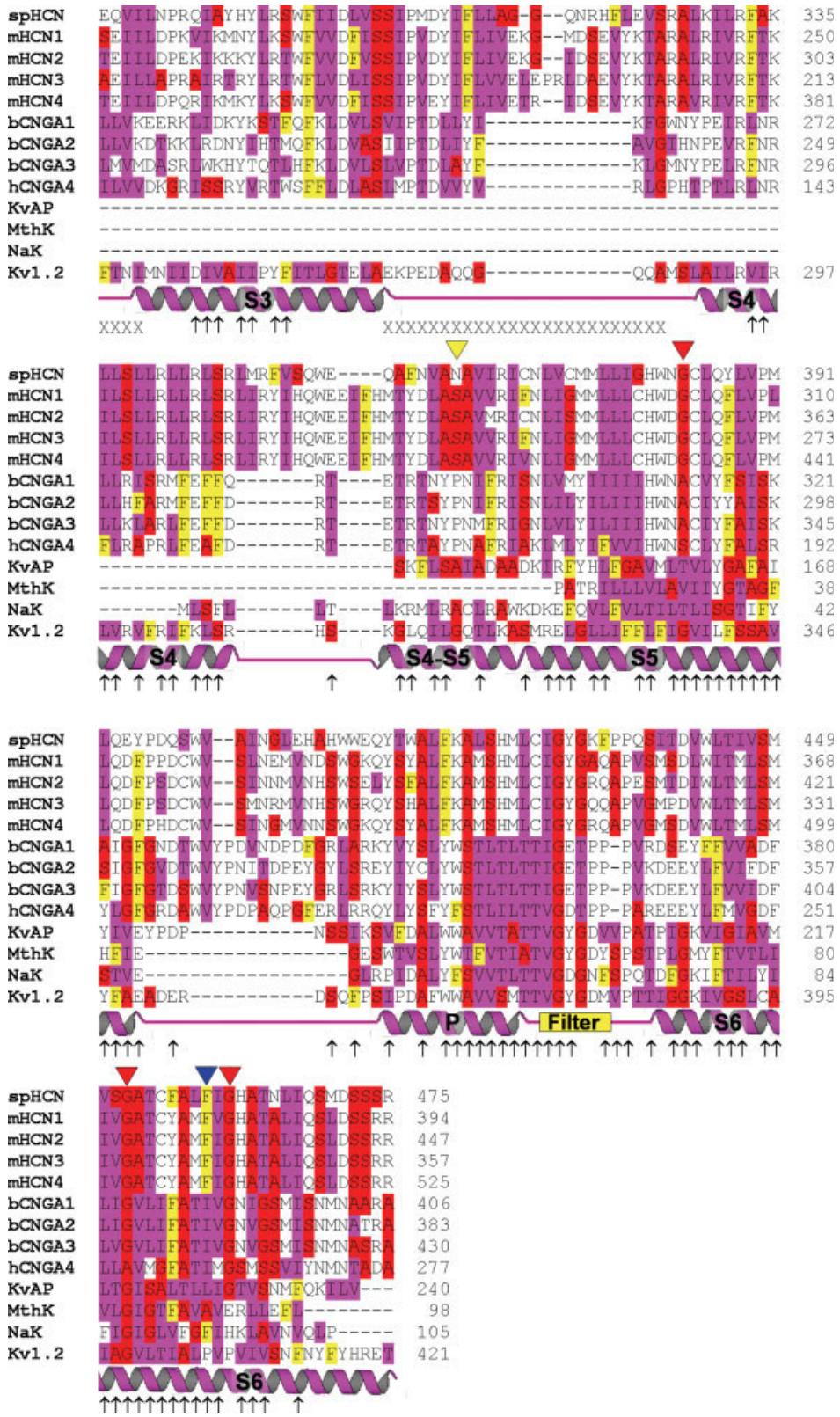

Fig. 3. Alignment of the sequences of spHCN, murine HCN1–4, bovine CNGA1–3, human CNGA4 and $K_v1.2$ channels. Sequence details are reported in the legend of Figure 2. Red represents Ala, Gly, and Ser; Ile, Leu, Thr, and Val residues are reported in purple; Phe are represented in yellow. The red arrows represent conserved glycines in S5 and S6 of HCN channels. The blue arrow represents F459 (spHCN notation). The yellow arrow represents the conserved P293 (bCNGA1 notation) of CNGA channels. The secondary structure annotation is that of $K_v1.2$ (the only crystallographic structure).[10] Buried amino acids in $K_v1.2$ are indicated by black arrows; X's indicate amino acids that are not present in $K_v1.2$ crystal structure.

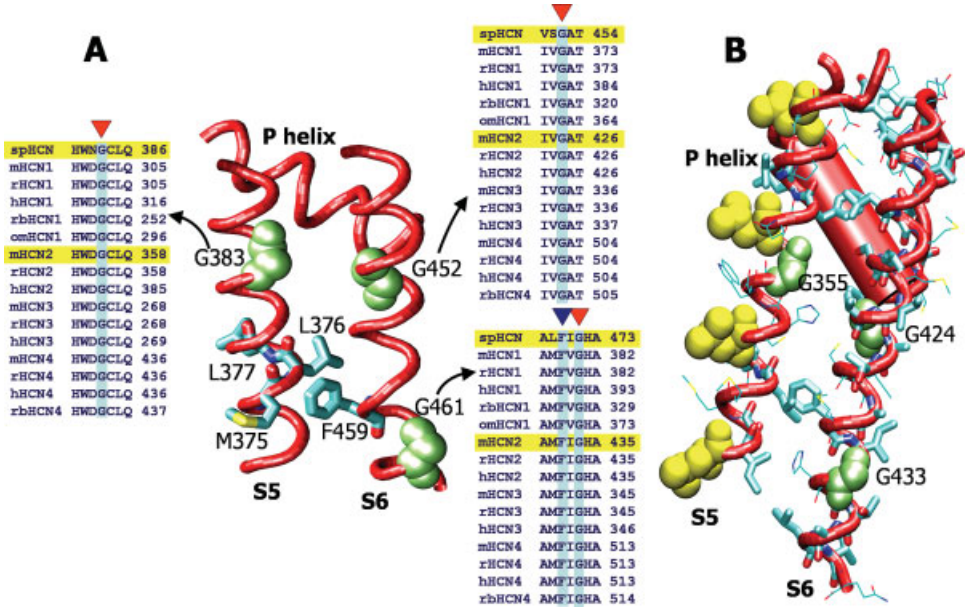

Fig. 4. (**A**) Model of the S5, S6, and P helices of spHCN. Glycines, which could be important for gating, G383, G452, and G461 are represented in green (van der Waals representation). F459 as well as the facing amino acids in S5 (M375, L376, and L377) are reported with bond representation. The sequence alignments of the regions, where G383, G452, F459, and G461 belong, are indicated by arrows. For clarity's sake, spHCN and mHCN2 sequence tracts are highlighted in yellow. (**B**) Model of the fragment from S5 to S6 of mHCN2. Ala, Ser, Ile, Leu, Phe, Thr, and Val residues are indicated by the bond representation. Conserved G355, G424, G433 (van der Waals representation) are indicated in green. L343, L350, L357, and L364, forming a leucine zipper, are shown in yellow (van der Waals representation). All the other amino acids in the S5 and S6 helices are reported with the line representation. [Color figure can be viewed in the online issue, which is available at www.interscience.wiley.com.]

membrane hyperpolarization and requires the presence of cAMP in order to open in a sustained way. However, normal gating is restored in the channel mutant F459L.[64]

The molecular model of the S5–S6 region of spHCN channel [Fig. 4(A)] shows that F459 faces L376 in the S5 helix, suggesting a possible interaction between leucines in the F459L mutant and, eventually, the coupling between S5 and S6.

The molecular model of S5–S6 of mHCN2 highlights the presence of a leucine zipper motif at S5 (L343, L350, L357, and L364), possibly mediating the channel assembly [Fig. 4(B)].

The S6 Domain

In HCN and CNG channels, the S6 domain is attached to a large CNB domain. Evidence provided in literature shows that ligand binding causes a conformational change in the CNB domains of both HCN[21,58,65] and CNG[21,58,66] channels, as well as in a prokaryotic cyclic nucleotide regulated channel.[67] These movements are eventually transmitted to the gate through the S6 domain and produce an increase of the open state probability in all these channels.

It is straightforward that the terminal motion of the S6 domain is restrained in HCN and CNG channels by the presence of the CNB domains. On the contrary, the C-terminal end of the S6 domain of the great majority of K^+ channels is not connected to large cytoplasmic domains and it is reasonable that it can move rather freely.

The PXP Motif in K^+ Channels

K^+ channels of the subfamilies from K_v1 to K_v4 form functional homotetrameric channels, while many K^+ channels of the subfamilies from K_v5 to K_v11 are not able to generate current by themselves, because of retention in the endoplasmatic reticulum (ER).[31,68–72]

A remarkable feature characterizes all K^+ channels of the K_v1–4 subfamilies: the highly conserved PXP motif.[31–35] The PXP motif is important for channel gating,[32,33] but it is not essential. S6 domain substitution of KcsA, lacking the PXP motif, inside a Shaker K_v channel indeed produced functional chimeric channels, but with an activation voltage considerably shifted toward more positive values.[73] As a result, the PXP motif seems to reduce the voltage depolarization necessary to open K^+ channels.

It is well known that prolines break α-helices[74–76] and that the PXP motif does actually introduce a kink of ~35° in S6 of $K_v1.2$ crystal structure.[10,11] Therefore, S6 in the PXP-containing K^+ channels is expected to have a significant outward bend also in the absence of external forces, i.e. at 0 mV. We hypothesize that K_v1–4 channels are in the open state (or in a very similar conformation) also in the absence of external electrical fields and an

appropriate force is necessary to push S6 in the closed conformation.

By contrast, no HCN and CNG channels have the PXP motif or even a single proline in S6. Therefore, in the absence of external electric fields and cyclic nucleotides, the S6 helix of CNG and HCN channels is expected to be in an unbroken α-helical conformation. In all HCN and CNG channels, S6 features two very flexible glycines (red arrows in Figs. 3 and 4), which are the putative hinges for gating.[27,29,36–38] As a consequence, the S6 domain can bend in the presence of external forces (analogously to MthK in the open conformation),[37,38] exerted either by conformational changes of the CNB domain in CNG and HCN channels or by an external electric field in HCN channels.

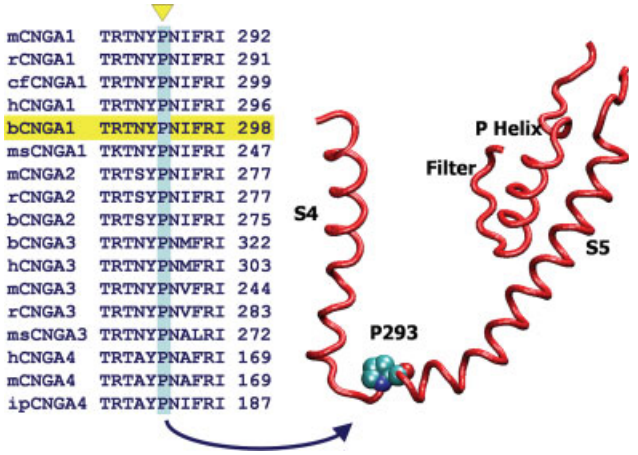

Fig. 5. Model of fragment from S4 to the selectivity filter for bCNGA1. The conserved P293 is indicated by the van der Waals representation and indicated by the yellow arrow in the sequence alignments of the corresponding region. For clarity's sake, bCNGA1 sequence is highlighted in yellow. [Color figure can be viewed in the online issue, which is available at www.interscience.wiley.com.]

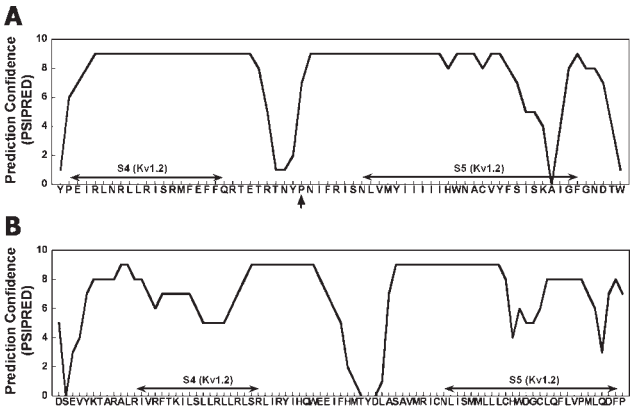

Fig. 6. (**A**, **B**) Helix prediction confidence calculated with PSIPRED server[47] for the putative tract containing S4 and S5 of bCNGA1 (**A**) and mHCN2 (**B**). In panel A, the arrow represents P293.

The S5 Domain

The S5 domain of HCN channels has a conserved glycine in the middle of the helix (Figs. 3 and 4). In 3-D structural models of the S5-P-filter-S6 region (Fig. 4), this glycine is located at the same height of one of the two glycines present in the S6 domain (for instance G424 of the mHCN2 channel). Therefore, the presence of the two glycines in the middle of S5 and S6 could constitute the hinge around which a concerted motion of S5 and S6 could occur, allowing the lower parts of the two α-helices to move in a coordinated way.

As aforementioned, the F459L spHCN mutant recovers the normal gating behavior of HCN channels, which can open in a sustained way also in the absence of cyclic nucleotides.[64] This mutation could form leucine zippers between S5 and S6 [Fig. 4(A)], suggesting the necessity of a tight coupling between S5 and S6 for the usual gating of HCN channels. It should be noted that a glycine is also present in K_v1.2 S5 (G338), but no appreciable kinks are visible in the helix in the channel open conformation. On the contrary, no glycines are present in the S5 domains of CNG channels. Therefore, there are no hints that a similar mechanism would also be valid for these channels.

The S4–S5 Linker

In the crystal structure of K_v1.2,[10,11] helices S4 and S5 are connected by a linker, called S4–S5, composed of about 14 residues forming an α-helix. This linker is quite likely to play a major role in the gating of K^+ channels as a downward displacement of the S4 helix of just a few angstroms pushes down the S4–S5 linker, which is rigid enough to compress the C-terminal end of S6 and lead to the channel closure.[11] As shown in Figure 3, the S4–S5 linker sequences are different in K_v1.2, CNG, and HCN channels: CNG channels have a shorter linker composed of about 11 residues, with one proline (P293 in bCNGA1 notation) in the middle. This proline is conserved in almost all CNGA 1–4 subunits from different species (Fig. 5). In addition, CNG channels lack many of the residues with a high α-helical interface propensity, which are present in the other channels of this region (Fig. 3). Secondary structure predictions show that the segment T[NSA]YP of the S4–S5 linker of CNGA 1–4 channels is unlikely in an α-helical conformation [Fig. 6(A)], but it could be a flexible loop (Fig. 5), therefore decoupling the movements of the voltage sensor S4 and the S6 helix.

The linker region of HCN channels is significantly longer than in K_v1.2 by about 13 residues, but secondary structure predictions again suggest the α-helical conformation are unlikely [Fig. 6 (B)]. On the contrary, they predict that S4 helix ends at E325 whereas the S5 helix should start at S335 (mHCN2 notation). This is also supported by the good propensity of the glutamic acid and serine for C- and N-capping in α-helices, respectively,[77–79] suggesting the notion that in HCN channels, the S5 helix could be longer than in K_v1.2 (and CNG channels). Algorithms for the detection of possible kinks and bends in α

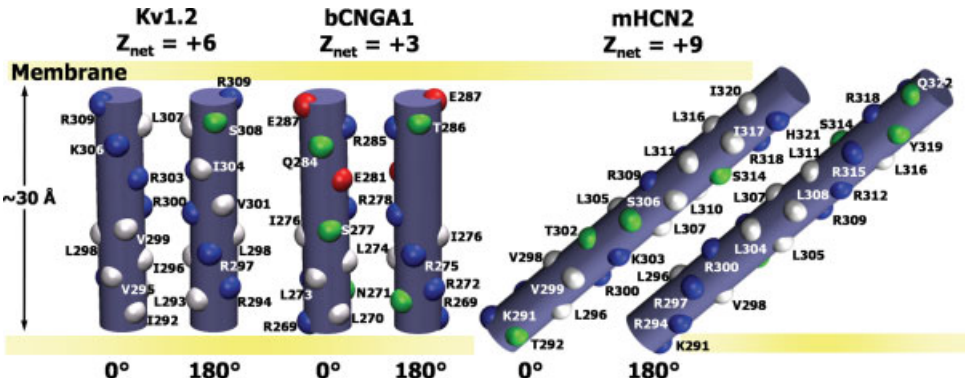

Fig. 7. Comparison between the helices S4 in K_v1.2, bCNGA1, and mHCN2, as interfered by the sequence alignment. For clarity reasons, helices are depicted as cylinders, rotated by 180° around their symmetry axes. Important residues are mapped on the helices with different colors: red, blue, and green indicate acid, basic, and polar amino acids, respectively. White represents Ile, Leu, and Val. [Color figure can be viewed in the online issue, which is available at www.interscience.wiley.com.]

helices[80] do not predict any significant deviation from the α-helix conformation in this region (data not shown).

The S4 Domain: The Voltage Sensor

The motif a^+bc, consisting of a positively charged residue, either an arginine or a lysine, separated by two hydrophobic residues, is present in CNG, HCN, and K^+ channels but with some differences (Figs. 3 and 7). In the great majority of K^+ channels, the motif appears six times with a net charge of +6. In CNG channels, it is repeated five times, but the presence of two glutamic acids leads to a net charge of +3. In HCN channels, the same motif is present nine times, with a net charge of +9. These structural differences of S4 were expected, given the different voltage sensitivity of K_v1.2, CNG, and HCN channels.

The voltage sensor of HCN channels is also very rich in leucines and isoleucines, with several pairs of leucines separating two positively charged residues. This could be due to both a tight coupling between S4 and the other domains of the channels (i.e. S5 and/or S6) by means of heptad repeats and the necessity of making the S4 helix more hydrophobic, in order to allow positive residues to lie inside the membrane. In fact, leucines and isoleucines are among the foremost hydrophobic amino acids.[81] In addition, the presumed S4 helix of HCN channels appears significantly longer (~33 amino acids). Given the high number of hydrophobic residues, this domain is expected to remain almost entirely in the membrane during gating. Prediction algorithms[80] do not suggest the presence of kinks or other modifications inside the α-helix (data not shown). Therefore, we hypothesize the S4 domain in HCN channels to be more tilted than in K_v1.2 channels.

CONCLUSIONS

The present bioinformatic investigation has identified several motifs specific for all known members of K_v, CNG, and HCN channels, which are therefore expected to provide a rationale for understanding the functional diversity among these channels.

In spite of the low sequence identity, the sequence alignment of representative channels from different subfamilies resulted to be significant in the S5–S6 tract, because of the presence of a few channel signature sequences, the low expected structural divergence and the validation through cysteine mutagenesis experiments.[27,29] In addition, the presence of a^+bc patterns, consisting of a positively charged residue separated by two hydrophobic residues, easily permits the identification of the S4 helices in CNG and HCN channels. The sequence alignment of the other regions is less significative, as they are expected to be more structurally divergent. Therefore, we have limited our discussion to the S4–S6 domains. Here we summarize our findings and provide some functional implications.

1. The S6 helix of all functional voltage-gated K^+ channels, namely members of K_v 1–4 subfamilies, features the PXP motif.[35] In general, K^+ channels lacking this motif either are not voltage gated, such as KcsA,[40] or do not form functional homomeric channels.[31,68–72] The motif PXP is expected to introduce a kink in S6 helix, as seen in the crystal structure of K_v1.2.[10,11] By contrast, S6 in all known HCN and CNG channels lacks the PXP motif (Fig. 3). It features instead two highly conserved glycines (Figs. 3 and 4). These glycines are quite likely to be the hinges around which the motion of the S6 domain occurs during gating. Also S5 of HCN channels has one highly conserved glycine (Figs. 3 and 4), which could play a role during channel gating.[38] These findings can explain why HCN and CNG channels are usually in the closed conformation in the absence of external electric field and/or cyclic nucleotides.
2. The properties of S4 helix, i.e. the voltage sensor, differ for K_v, HCN and CNG channels (Fig. 7): S4 has a

net charge of +6 in K_v channels, +3 in CNG channels, while in HCN channels is +9. In addition, S4 in HCN channels appears to be significantly longer than in the HCN and K_v channels. Therefore, S4 net charge can partially explain the different voltage sensitivity of K_v1.2, CNG, and HCN channels.

3. The S4–S5 linker region of all CNGA channels features a conserved proline, which is absent in HCN and K_v channels (Fig. 5). This proline is likely to reduce the mechanical coupling between S4, S5, and S6 helices, which could occur during the gating process of usual voltage-gated K^+ channels.
4. Amino acids with a high propensity for α-helical interfaces are present in the S4, S5, and S6 domains of all channels (Fig. 3). As a consequence, these domains are more likely to interact with each other and move in a concerted way during gating. In the case of voltage-gated K^+ channels, interfacial amino acids are located along the linker S4–S5 and the S5–S6 tract, and the possible role of the hydrophobic residues in this region for the gating has indeed been suggested both from mutagenesis experiments[63] and the analysis of K_v1.2 crystal structure.[11] Ser and Leu are more present in the S4 domain of HCN channels, suggesting that this helix is more mechanically coupled to the other domains than in K_v channels. In the case of CNG channels, a large number of amino acids with a high α-helical interface propensity are located in the P helix, but in this case it is difficult to advance if they have a functional role and which could it be.

At a speculative level, we can rationalize some of the different gating features of K_v, CNG, and HCN channels.

As for K_v channels, the PXP motif in the S6 domain induces S6 to bend in the absence of external forces. As the kink of S6 is known to be associated to the gating,[32] these channels are either in the open conformation or close to it even in the absence of the membrane depolarization. This can explain the observations that, in most cases, voltage-gated K^+ channels open when the membrane electrical potential approaches 0 mV and need the membrane to be hyperpolarized in order to close. The exact molecular mechanisms leading to the closure of K_v channels is still a matter of debate.

In the case of CNG channels, our bioinformatics considerations provide a rather clear rationale for explaining why CNG channels are poorly voltage dependent. First, the S4 domain has a lower net positive charge with respect to K_v channels. Second, the S4–S5 linker is shorter and probably forms a loop. Therefore, the motion of the S4 domain is not efficiently coupled to the S6 domain as in K_v and HCN channels. Finally, the PXP motif is absent in the S6 domain, whose end portion is constrained by the large cytoplasmic domain.

As for HCN channels, our investigations can provide some hints on the gating and in particular why they open at negative voltages and with a significantly longer time constant with respect to voltage-gated K^+ channels (~100 times longer). Analogously to K_v channels, the opening of HCN channels is associated to an outward bending of the S6 domain,[29] which is initiated by the downward motion of the S4 domain.[8] The presence of extensive repeats of leucines and other amino acids with similar packing properties suggests that gating occurs through a coordinated motion of S4, which acts on the S6 and, probably, the S5 domains. Therefore, the whole process is expected to be slowed down considerably by all the necessary conformational changes. By contrast, domains in K_v channels are expected to move relatively more freely, consistently with a faster gating.

The proposed role as hinges of the prolines in the PXP motif in K^+ channels and of glycines in CNG and HCN channels are in agreement with the available experimental evidences. In particular, the comparisons of the crystal structures of closed and open K^+ channels[9–11,28,37,38,40,42] clearly shows the bending of the S6 transmembrane helix around either the PXP motif[10,11] (where present) or a glycine.[9,37,38] G395 of bCNGA1 is quite likely to behave as a hinge during gating as previously suggested.[82,83] The notion that G461 in spHCN acts as a hinge in HCN channels is consistent with the available electrophysiological analysis[84] and a detailed modelling of gating in HCN channels.[29]

In conclusion, we have advanced, at a qualitative level, some explanations about the molecular mechanisms that cause the gating of CNG channels to be poorly voltage dependent, in contrast to voltage-gated channels. We have also provided some hints on why HCN channels open at negative voltages and with slow kinetics. These findings can be tested by appropriate experiments with engineered channels; in particular, in the light of our discussion, it would be highly interesting to analyze the role of the proline in the S4–S5 linker of CNG channels and that of the leucines in the S4 domain of HCN channels.

ACKNOWLEDGMENTS

The authors thank Graeme M. Robertson (Siena Biotech, Italy) for the useful suggestions and for reading the manuscript. CA thanks Barbara Ciani (Wellcome Trust Centre for Cell Matrix Research, Manchester, UK) for the useful suggestions and discussions about "coiled coils" motifs.

REFERENCES

1. Hille B. Ion channels of excitable membranes. Sunderland, MA: Sinauer; 2001.
2. Jan LY, Jan YN. How might the diversity of potassium channels be generated? Trends Neurosci 1990;13:415–419.
3. Hodgkin AL, Huxley AF. Currents carried by sodium and potassium ions through the membrane of the giant axon of Loligo. J Physiol 1952;116:449–472.
4. Miller C. An overview of the potassium channel family. Genome Biol 2000;1: Reviews 0004.
5. Seoh SA, Sigg D, Papazian DM, Bezanilla F. Voltage-sensing residues in the S2 and S4 segments of the Shaker K^+ channel. Neuron 1996;16:1159–1167.

6. Mannuzzu LM, Moronne MM, Isacoff EY. Direct physical measure of conformational rearrangement underlying potassium channel gating. Science 1996;271:213–216.
7. Aggarwal SK, MacKinnon R. Contribution of the S4 segment to gating charge in the Shaker K^+ channel. Neuron 1996;16:1169–1177.
8. Männikkö R, Elinder F, Larsson HP. Voltage-sensing mechanism is conserved among ion channels gated by opposite voltages. Nature 2002;419:837–841.
9. Jiang Y, Lee A, Chen J, Ruta V, Cadene M, Chait BT, MacKinnon R. X-ray structure of a voltage-dependent K^+ channel. Nature 2003;423:33–41.
10. Long SB, Campbell EB, MacKinnon R. Crystal structure of a mammalian voltage-dependent Shaker family K^+ channel. Science 2005;309:897–903.
11. Long SB, Campbell EB, MacKinnon R. Voltage sensor of Kv1.2: structural basis of electromechanical coupling . Science 2005;309:903–908.
12. Posson DJ, Ge P, Miller C, Bezanilla F, Selvin PR. Small vertical movement of a K^+ channel voltage sensor measured with luminescence energy transfer. Nature 2005;436:848–851.
13. Phillips LR, Milescu M, Li-Smerin Y, Mindell JA, Kim JI, Swartz KJ. Voltage-sensor activation with a tarantula toxin as cargo. Nature 2005;436:857–860.
14. Chanda B, Asamoah OK, Blunck R, Roux B, Bezanilla F. Gating charge displacement in voltage-gated ion channels involves limited transmembrane movement. Nature 2005;436:852–856.
15. Noda M, Shimizu S, Tanabe T, Takai T, Kayano T, Ikeda T, Takahashi H, Nakayama H, Kanaoka Y, Minamino N. Primary structure of electrophorus electricus sodium channel deduced from cDNA sequence. Nature 1984;312:121–127.
16. Tanabe T, Takeshima H, Mikami A, Flockerzi V, Takahashi H, Kangawa K, Kojima M, Matsuo H, Hirose T, Numa S. Primary structure of the receptor for calcium channel blockers from skeletal muscle. Nature 1987;328:313–318.
17. Tempel BL, Papazian DM, Schwarz TL, Jan YN, Jan LY. Sequence of a probable potassium channel component encoded at Shaker locus of *Drosophila*. Science 1987;237:770–775.
18. Fesenko EE, Kolesnikov SS, Lyubarsky AL. Induction by cyclic GMP of cationic conductance in plasma membrane of retinal rod outer segment. Nature 1985;313:310–313.
19. Zimmerman AL, Baylor DA. Cyclic GMP-sensitive conductance of retinal rods consists of aqueous pores. Nature 1986;321:70–72.
20. Nakamura T, Gold GH. A cyclic nucleotide-gated conductance in olfactory receptor cilia. Nature 1987;325:442–444.
21. Craven KB, Zagotta WN. Salt bridges and gating in the COOH-terminal region of HCN2 and CNGA1 channels. J Gen Physiol 2004;124:663–677.
22. Halliwell JV, Adams PR. Voltage-clamp analysis of muscarinic excitation in hippocampal neurons. Brain Res 1982;250:71–92.
23. DiFrancesco D. Pacemaker mechanisms in cardiac tissue. Annu Rev Physiol 1993;55:455–472.
24. Brown H, Ho W.The hyperpolarization-activated inward channel and cardiac pacemaker activity. In: Morad M, Ebashi S, Trautwein W, Kurachi Y, editors. Molecular physiology and pharmacology of cardiac ion channels and transporters. Dordrecht, The Netherlands: Kluwer; 1996.30p.
25. Pape HC. Queer current and pacemaker: the hyperpolarization-activated cation current in neurons. Annu Rev Physiol 1996;58:299–327.
26. Zagotta WN, Olivier NB, Black KD, Young EC, Olson R, Gouaux E. Structural basis for modulation and agonist specificity of HCN pacemaker channels. Nature 2003;425:200–205.
27. Giorgetti A, Nair AV, Codega P, Torre V, Carloni P. Structural basis of gating of CNG channels. FEBS Lett 2005;579:1968–1972.
28. Shi N, Ye S, Alam A, Chen L, Jiang Y. Atomic structure of a Na^+- and K^+-conducting channel. Nature 2006;440:570–574.
29. Giorgetti A, Carloni P, Mistrik P, Torre V. A homology model of the pore region of HCN channels. Biophys J 2005;89:932–944.
30. Nair AV, Mazzolini M, Codega P, Giorgetti A, Torre V. Locking CNGA1 channels in the open and closed state. Biophys J 2006;90:3599–3607.
31. Ottschytsch N, Raes A, Van Hoorick D, Snyders DJ. Obligatory heterotetramerization of three previously uncharacterized Kv channel α-subunits identified in the human genome. Proc Natl Acad Sci USA 2002;99:7986–7991.
32. Labro AJ, Raes AL, Bellens I, Ottschytsch N, Snyders DJ. Gating of shaker-type channels requires the flexibility of S6 caused by prolines. J Biol Chem 2003;278:50724–50731.
33. Harris T, Graber AR, Covarrubias M. Allosteric modulation of a neuronal K^+ channel by 1-alkanols is linked to a key residue in the activation gate. Am J Physiol Cell Physiol 2003;285:C788–C796.
34. Kerschensteiner D, Monje F, Stocker M. Structural determinants of the regulation of the voltage-gated potassium channel Kv2.1 by the modulatory α-subunit Kv9.3. J Biol Chem 2003;278:18154–18161.
35. Ottschytsch N, Raes AL, Timmermans JP, Snyders DJ. Domain analysis of Kv6.3, an electrically silent channel. J Physiol 2005;568:737–747.
36. Ding S, Ingleby L, Ahern CA, Horn R. Investigating the putative glycine hinge in Shaker potassium channel. J Gen Physiol 2005;126:213–226.
37. Jiang Y, Lee A, Chen J, Cadene M, Chait BT, MacKinnon R. Crystal structure and mechanism of a calcium-gated potassium channel. Nature 2002;417:515–522.
38. Jiang Y, Lee A, Chen J, Cadene M, Chait BT, MacKinnon R. The open pore conformation of potassium channels. Nature 2002;417:523–526.
39. Yang N, George AL Jr, Horn R. Molecular basis of charge movement in voltage-gated sodium channels. Neuron 1996;16:113–122.
40. Doyle DA, Morais CJ, Pfuetzner RA, Kuo A, Gulbis JM, Cohen SL, Chait BT, MacKinnon R. The structure of the potassium channel: molecular basis of K^+ conduction and selectivity. Science 1998;280:69–77.
41. Zhou Y, Morais-Cabral JH, Kaufman A, MacKinnon R. Chemistry of ion coordination and hydration revealed by a K^+ channel-Fab complex at 2.0 A resolution. Nature 2001;414:43–48.
42. Kuo A, Gulbis JM, Antcliff JF, Rahman T, Lowe ED, Zimmer J, Cuthbertson J, Ashcroft FM, Ezaki T, Doyle DA. Crystal structure of the potassium channel KirBac1.1 in the closed state. Science 2003;300:1922–1926.
43. Russell RB, Barton GJ. Multiple protein sequence alignment from tertiary structure comparison: assignment of global and residue confidence levels. Proteins 1992;14:309–323.
44. Barton GJ, Sternberg MJ. A strategy for the rapid multiple alignment of protein sequences. Confidence levels from tertiary structure comparisons. J Mol Biol 1987;198:327–337.
45. Barton GJ. Protein multiple sequence alignment and flexible pattern matching. Methods Enzymol 1990;183:403–428.
46. Barton GJ, Sternberg MJ. Evaluation and improvements in the automatic alignment of protein sequences. Protein Eng 1987;1:89–94.
47. Jones DT. Protein secondary structure prediction based on position-specific scoring matrices. J Mol Biol 1999;292:195–202.
48. Hubbard SJ, Thornton JM. NACCESS. London: Department of Biochemistry and Molecular Biology, University College; 1993.
49. Šali A, Blundell TL. Comparative protein modelling by satisfaction of spatial restraints. J Mol Biol 1993;234:779–815.
50. Kaupp UB, Niidome T, Tanabe T, Terada S, Bonigk W, Stuhmer W, Cook NJ, Kangawa K, Matsuo H, Hirose T. Primary structure and functional expression from complementary DNA of the rod photoreceptor cyclic GMP-gated channel. Nature 1989;342:762–766.
51. Dhallan RS, Yau KW, Schrader KA, Reed RR. Primary structure and functional expression of a cyclic nucleotide-activated channel from olfactory neurons. Nature 1990;347:184–187.
52. Weyand I, Godde M, Frings S, Weiner J, Muller F, Altenhofen W, Hatt H, Kaupp UB. Cloning and functional expression of a cyclic-nucleotide-gated channel from mammalian sperm. Nature 1994;368:859–863.
53. Bradley J, Li J, Davidson N, Lester HA, Zinn K. Heteromeric olfactory cyclic nucleotide-gated channels: a subunit that confers increased sensitivity to cAMP. Proc Natl Acad Sci USA 1994;91:8890–8894.
54. Liman ER, Buck LB. A second subunit of the olfactory cyclic nucleotide-gated channel confers high sensitivity to cAMP. Neuron 1994;13:611–621.
55. Gerstner A, Zong X, Hofmann F, Biel M. Molecular cloning and functional characterization of a new modulatory cyclic nucleotide-gated channel subunit from mouse retina. J Neurosci 2000;20:1324–1332.

56. Cheng KT, Chan FL, Huang Y, Chan WY, Yao X. Expression of olfactory-type cyclic nucleotide-gated channel (CNGA2) in vascular tissues. Histochem Cell Biol 2003;120:475–481.
57. Craven KB, Zagotta WN. CNG and HCN channels: two peas, one pod. Annu Rev Physiol 2006;68:375–401.
58. Zhou L, Olivier NB, Yao H, Young EC, Siegelbaum SA. A conserved tripeptide in CNG and HCN channels regulates ligand gating by controlling C-terminal oligomerization. Neuron 2004;44: 823–834.
59. Eilers M, Patel AB, Liu W, Smith SO. Comparison of helix interactions in membrane and soluble α-bundle proteins. Biophys J 2002;82:2720–2736.
60. Burkhard P, Stetefeld J, Strelkov SV. Coiled coils: a highly versatile protein folding motif. Trends Cell Biol 2001;11:82–88.
61. Gruber M, Lupas AN. Historical review: another 50th anniversary-new periodicities in coiled coils. Trends Biochem Sci 2003;28: 679–685.
62. Landschulz WH, Johnson PF, McKnight SL. The leucine zipper: a hypothetical structure common to a new class of DNA binding proteins. Science 1988;240:1759–1764.
63. McCormack K, Tanouye MA, Iverson LE, Lin J-W, Ramaswami M, McCormack T, Campanelli JT, Mathew MK, Rudy B. A role for hydrophobic residues in the voltage-dependent gating of Shaker K^+ channels. Proc Natl Acad Sci USA 1991;88:2931–2935.
64. Shin KS, Maertens C, Proenza C, Rothberg BS, Yellen G. Inactivation in HCN channels results from reclosure of the activation gate: desensitization to voltage. Neuron 2004;41:737–744.
65. Ulens C, Siegelbaum SA. Regulation of hyperpolarization-activated HCN channels by cAMP through a gating switch in binding domain symmetry. Neuron 2003;40:959–970.
66. Hua L, Gordon SE. Functional interactions between A' helices in the C-linker of open CNG channels. J Gen Physiol 2005;125: 335–344.
67. Clayton GM, Silverman WR, Heginbotham L, Morais-Cabral JH. Structural basis of ligand activation in a cyclic nucleotide regulated potassium channel. Cell 2004;119:615–627.
68. Drewe JA, Verma S, Frech G, Joho RH. Distinct spatial and temporal expression patterns of K^+ channel mRNAs from different subfamilies. J Neurosci 1992;12:538–548.
69. Hugnot JP, Salinas M, Lesage F, Guillemare E, de Weille J, Heurteaux C, Mattei MG, Lazdunski M. Kv8.1, a new neuronal potassium channel subunit with specific inhibitory properties towards Shab and Shaw channels. EMBO J 1996;15:3322–3331.
70. Patel AJ, Lazdunski M, Honore E. Kv2.1/Kv9.3, a novel ATP-dependent delayed-rectifier K^+ channel in oxygen-sensitive pulmonary artery myocytes. EMBO J 1997;16:6615–6625.
71. Salinas M, Duprat F, Heurteaux C, Hugnot JP, Lazdunski M. New modulatory α subunits for mammalian Shab K^+ channels. J Biol Chem 1997;272:24371–24379.
72. Zhu XR, Netzer R, Bohlke K, Liu Q, Pongs O. Structural and functional characterization of Kv6.2 a new γ-subunit of voltage-gated potassium channel. Receptors Channels 1999;6:337–350.
73. Lu Z, Klem AM, Ramu Y. Ion conduction pore is conserved among potassium channels. Nature 2001;413:809–813.
74. Barlow DJ, Thornton JM. Helix geometry in proteins. J Mol Biol 1988;201:601–619.
75. von Heijne G. Proline kinks in transmembrane α-helices. J Mol Biol 1991;218:499–503.
76. Sankararamakrishnan R, Vishveshwara S. Geometry of proline-containing α-helices in proteins. Int J Pept Protein Res 1992;39: 356–363.
77. Doig AJ, Baldwin RL. N- and C-capping preferences for all 20 amino acids in α-helical peptides. Protein Sci 1995;4:1325–1336.
78. Doig AJ, MacArthur MW, Stapley BJ, Thornton JM. Structures of N-termini of helices in proteins. Protein Sci 1997;6: 147–155.
79. Cochran DA, Penel S, Doig AJ. Effect of the N1 residue on the stability of the α-helix for all 20 amino acids. Protein Sci 2001;10:463–470.
80. Rigoutsos I, Riek P, Graham RM, Novotny J. Structural details (kinks and non-α conformations) in transmembrane helices are intrahelically determined and can be predicted by sequence pattern descriptors. Nucleic Acids Res 2003;31:4625–4631.
81. White SH, Wimley WC. Membrane protein folding and stability: physical principles. Annu Rev Biophys Biomol Struct 1999;28: 319–365.
82. Flynn GE, Zagotta WN. Conformational changes in S6 coupled to the opening of cyclic nucleotide-gated channels. Neuron 2001;30: 689–698.
83. Flynn GE, Zagotta WN. A cysteine scan of the inner vestibule of cyclic nucleotide-gated channels reveals architecture and rearrangement of the pore. J Gen Physiol 2003;121:563–582.
84. Rothberg BS, Shin KS, Phale PS, Yellen G. Voltage-controlled gating at the intracellular entrance to a hyperpolarization-activated cation channel. J Gen Physiol 2002;119:83–91.